Available online at www.sciencedirect.com
SCIENCE DIRECT
Developmental Biology 290 (2006) 337 – 350
DEVELOPMENTAL BIOLOGY
www.elsevier.com/locate/ydbio

Specification of neural precursor identity in the geophilomorph centipede *Strigamia maritima*

Ariel D. Chipman [1], Angelika Stollewerk *,[1]

Department of Zoology, University of Cambridge, Downing Street, Cambridge CB2 3EJ, UK

Received for publication 24 June 2005, revised 14 November 2005, accepted 15 November 2005
Available online 27 December 2005

Abstract

Despite differences in the formation of neural precursors, all arthropod species analyzed so far generate about 30 single precursors (insects/crustaceans) or precursor groups (chelicerates/myriapods) per hemi-segment. In *Drosophila*, each precursor has a distinct identity conferred by segment polarity and dorso-ventral patterning genes that subdivide the ventral neuroectoderm into a grid-like structure. Temporal patterning mechanisms generate additional diversity after delamination from the neuroectoderm. Previous work shows that the genetic network involved in recruitment and specification of neural precursors is conserved in arthropods. However, comparative studies on generation of precursor diversity are few and partial. Here, we test whether aspects of the *Drosophila* model may apply in the geophilomorph centipede *Strigamia maritima*. We describe precursor formation, based on morphology and on *Delta* and *Notch* expression. We then show that in *S. maritima*, *hunchback* and *Krüppel* are expressed in subsets of neural precursors generating distinct temporal expression domains within the plane of the neuroectoderm. This expression pattern suggests that temporal changes in spatial patterning cues may result in the ordered production of different neural identities. We suggest that temporal patterning mechanisms were present in the last common ancestor of arthropods, although the regulatory interactions of transcription factors might have diverged in the lineage leading to insects.

Keywords: Neurogenesis; Precursor identity; Arthropod; Myriapod; Temporal identity

Introduction

Generation of neural precursor diversity is a crucial early stage in the patterning of the nervous system. Comparing this process in different taxa can shed light on the evolution of nervous systems, and help identify the direction of evolutionary change within and between major taxonomic groups. There are at present two competing views as to the relationship between the major arthropod groups. A group uniting the chelicerates and myriapods (the Myriochelata) has recently been suggested based on molecular data (Friedrich and Tautz, 1995; Hwang et al., 2001; Kusche and Burmester, 2001; Nardi et al., 2003; Mallatt et al., 2004; Pisani et al., 2004). This grouping is supported by comparative analysis of neurogenesis in the chelicerate *Cupiennius salei* (a spider) and the myriapods *Lithobius forficatus* (a centipede) and *Glomeris marginata* (a millipede) (Stollewerk, 2002; Stollewerk et al., 2001; Dove and Stollewerk, 2003; Stollewerk et al., 2003; Kadner and Stollewerk, 2004). Several characters have been described that cannot be found in equivalent form in the remaining arthropod groups, insects, and crustaceans. (1) Groups of neural precursors invaginate from the ventral neuroectoderm of chelicerates and myriapods, while single neural precursors are specified in insects and crustaceans. (2) In contrast to insects and crustaceans, neural precursors do not divide in a stem cell-like mode in chelicerates and myriapods. (3) The central region of the ventral neuroectoderm in chelicerates and myriapods generates exclusively neural cells, while in insects and crustaceans both neural and epidermal cells arise from the ventral neurogenic region. It is possible that these characters are shared derived characters (synapomorphies) of myriapods and chelicerates, providing the first morphological support for a clade uniting these two groups. However, they could also represent ancestral characters (sympleisiomorphies) retained in myriapods and chelicerates and lost in the more derived insects

* Corresponding author. Present address: Johannes-Gutenberg University Mainz, Department of Genetics, Johann-Joachim-Becherweg 32, 55099 Mainz, Germany. Fax: +44 1223 336676.
E-mail address: stollewe@uni-mainz.de (A. Stollewerk).

0012-1606/$ - see front matter © 2005 Elsevier Inc. All rights reserved.
doi:10.1016/j.ydbio.2005.11.029

and crustaceans. This would be consistent with the competing (and traditional) view of insects and crustaceans forming a single clade, the Tetraconata (or Pancrustacea), with myriapods as a sister group to that clade (the Mandibulata hypothesis). Analyses of neurogenesis in outgroups to the Euarthropoda, the onychophorans, and tardigrades at the moment fail to resolve this conflict: invaginating neural precursor groups have not been described in these outgroups (Eriksson et al., 2003) (personal communication, A. Hejnol). However, only two, possibly derived, species have been analyzed that may not represent the ancestral state.

We aim to broaden our understanding of nervous development in basal arthropod groups and reconstruct the ancestral state of neurogenesis. It can be assumed that characters that are conserved in all arthropod groups were present in the last common ancestor. In this paper, we analyze an additional myriapod, the geophilomorph centipede *Strigamia maritima*. Unlike other species of myriapods that have been used previously for the study of neural development (Dove and Stollewerk, 2003; Kadner and Stollewerk, 2004), *S. maritima* forms all of its segments during embryogenesis, a mode of embryogenesis known as epimorphic development. In contrast, in previously studied species, only a small number of segments are formed during embryonic development, and additional segments are added in successive moults (anamorphic development). *S. maritima* has 47–53 leg-bearing segments. Segments are added sequentially from a posterior undifferentiated disk throughout the segmentation process. Therefore, there is an anterior–posterior gradient in the developmental stage of individual segments, with anterior segments being more advanced than posterior ones. Due to this temporal gradient, we can follow dynamic processes by looking at a single specimen and observing a sequence of developmental events as they occur in successive segments.

In the insect *Drosophila melanogaster*, the competence to adopt neural fate depends on the presence of the proneural genes *achaete*, *scute*, and *lethal of scute*. At the beginning of neurogenesis, these genes are expressed in clusters of cells in each hemi-segment. During specification of neuroblasts, proneural gene expression becomes restricted to a single cell of the cluster, the future neuroblast (Cabrera et al., 1987; Romani et al., 1987; Skeath et al., 1992). This process is called lateral inhibition and is mediated by the neurogenic genes *Notch* and *Delta* (Simpson, 1990; Martin-Bermudo et al., 1995; Heitzler et al., 1996; Seugnet et al., 1997). The remaining cells of the cluster become epidermal, so that in *D. melanogaster*, both neural and ectodermal cells arise from the ventral neuroectoderm (Jiménez and Campos-Ortega, 1979; Cabrera et al., 1987; Jiménez and Campos-Ortega, 1990). Although there are differences in the formation of neural precursors, all arthropod species analyzed generate about 20 to 30 single neural precursors (insects/crustaceans) or precursor groups (chelicerates/myriapods) per hemi-segment that are arranged in 7 rows (Bate, 1976; Scholtz, 1992; Broadus and Doe, 1995; Gerberding, 1997; Harzsch, 2001; Stollewerk, 2002; Stollewerk et al., 2001, 2003; Dove and Stollewerk, 2003; Harzsch, 2003; Kadner and Stollewerk, 2004; Withington, 2004; Wheeler and Skeath, 2005; Wheeler et al., 2003). Furthermore, the genetic network involved in recruitment and specification of neural precursors is conserved in all arthropods that have been analyzed (Hartenstein and Campos-Ortega, 1984; Cabrera, 1990; Cabrera et al., 1987; Jiménez and Campos-Ortega, 1990; Simpson, 1990; Martin-Bermudo et al., 1991, 1995; Goodman and Doe, 1993; Heitzler et al., 1996; Seugnet et al., 1997; Stollewerk, 2002; Stollewerk et al., 2001, 2003; Dove and Stollewerk, 2003; Wheeler and Skeath, 2005; Wheeler et al., 2003; Kadner and Stollewerk, 2004). These data suggest that the regular arrangement of neural precursors as well as the genetic interactions that lead to recruitment of neurectodermal cells for neural fate were present in the last common ancestor of the arthropods.

However, comparative studies of the events that generate neural precursor diversity, following the recruitment of neural precursors, during early development of the ventral nerve cord in the different arthropod groups are few and incomplete (Stollewerk and Simpson, 2005). It has been shown in the insect *D. melanogaster* that once the neural precursors are selected they divide in a unique and invariant pattern generating a stereotyped sequential series of ganglion mother cells (GMC) (Doe and Goodman, 1992). Each GMC divides once to give rise to two neurons. Neural precursor diversity in *Drosophila* is achieved by both spatial and temporal patterning mechanisms. During neurogenesis, segment polarity and dorso-ventral patterning genes subdivide the ventral neuroectoderm into a grid-like structure (reviewed by Skeath, 1999). Each proneural cluster thus expresses a unique set of genes giving rise to neuroblasts with spatial heterogeneity. After delamination from the ventral neuroectoderm, neuroblasts become independent of spatial patterning cues. Subsequently, temporal patterning mechanisms generate additional diversity among the cell-lineages of individual neuroblasts. Kambadur et al. (1998) and Isshiki et al. (2001) demonstrated that temporal identity in neuroblasts is regulated by sequential expression of Hunchback, Krüppel, Pdm, and Castor. The temporal expression profile is maintained in the progeny of the neuroblasts leading to expression of transcription factors in mutually exclusive cell layers in the ventral neuromeres. *Hunchback* is expressed in early-born neurons that are located in the deepest layer, while *Krüppel* is expressed at low levels in the *Hunchback* layer and in a distinct layer between *Hunchback* and *Pdm*. *Castor* transcripts accumulate in the late-born superficial layer neurons.

We have shown previously that the expression of the segment polarity gene *engrailed* in neural precursors is conserved in chelicerates and myriapods suggesting that spatial patterning mechanisms similar to those of *Drosophila* generate heterogeneity among the neural precursors in the ventral neuroectoderm (Stollewerk and Chipman, in press). However, it is obvious that spatial information from segment polarity and dorso-ventral patterning genes alone cannot account for the high complexity of cell types in both groups. Counting mechanisms of the sort used by *Drosophila* neuroblasts could not operate in chelicerates and myriapods, since stem cell-like neuroblasts seem to be absent in these groups. Furthermore, the neural precursors are mainly postmitotic after invagination.

This raises the question of how sufficient neural diversity is generated in chelicerates and myriapods. We address this question here by analyzing the generation of neural precursors and genes that might be involved in the establishment of their identity in the geophilomorph centipede *S. maritima*.

Material and methods

Embryonic material

Embryos of *S. maritima* were collected and fixed in Brora, northern Scotland, during June 2004, as described previously (Chipman et al., 2004b). In addition to material fixed in the field, some clutches were collected and returned to the lab live (Chipman et al., 2004b), and fixed in the lab for phalloidin labeling (see below).

RNA in situ hybridization

Single and double staining for RNA expression patterns were done essentially as described before (Chipman et al., 2004a). Two-color double staining followed the same procedure, but the quality of the staining was improved considerably by the following modifications; For both Digoxigenin-labeled and fluorescein-labeled probes, probe concentration was reduced to 0.5–1 μg/ml and staining times were increased, in some cases to overnight staining. The detection of the first probe by Fast Red (Roche) always preceded detection of the second probe by BM-Purple (Roche). The weaker of the two probes was used second (in contrast with most published protocols), because the BM-purple stain is more robust and gives significantly better signal/noise ratios. A further consideration was the size of the probe. Although in our hands, good signal was obtained from probes as small as 200 bp, for two-color stainings, the minimal probe length was 500 bp.

After staining, the embryo was removed from the yolk and flat-mounted on a microscope slide for observation. Embryos were photographed with a Leica DFC300F digital camera mounted on a Zeiss Axiophot microscope, and driven by Leica Firecam image acquisition software. The quality of the image was enhanced by using a high Gamma value (up to 2.5) during image acquisition. Because detecting with Fast-Red tends to stain embryonic tissue a pale orange (clearly distinct from the bright magenta of the actual reaction product), we set the white balance reference point on the orange stained embryonic tissue to further enhance image quality. Only minimal image processing with Adobe Photoshop was carried out following this procedure.

Gene cloning

Genes used in this study were cloned using a combination of methods, the specifics being determined empirically for each gene. Degenerate PCR was done either on genomic DNA or on cDNA made by priming total RNA with a hexanucleotide primer mix (Roche) and reverse transcribing with Expand Reverse Transcriptase (Roche) using the manufacturer's protocol. PCR fragments were expanded by inverse PCR or 5′ RACE (SMART RACE-BD Biosciences), using specific primers against sequences from the initial PCR fragment.

Delta

Degenerate primers were designed against conserved regions surrounding the DSL domain, using alignments of *Delta* sequences from *D. melanogaster*, *G. marginata*, *L. forficatus*, and *C. salei.* Positive results were obtained using the forward primer RVCLKHYQ (GRGTGTGGYTNAARCAYTAYCA) and the reverse primer WGGLFCNQ (TGGTTACAGAANARNCCNCCCCA). The resulting 670 bp RT-PCR fragment (including primers. GenBank accession AY995115) was used directly for in situ hybridization experiments.

Notch

A 395 bp fragment of *StmNotch* was cloned using the degenerate primers forward GKTKLLCH (GGNAARACNGGNYTNYTNTGYCA) and reverse PCQNGGTC (CANGTNCCNCCRTTYTGRCANGG). This sequence was extended using 5′ RACE to give an additional 604 bp fragment (GenBank accession AY995116). Attempts to clone out a longer fragment using the sequence data from the two available fragments were unsuccessful due to the highly repetitive nature of the EGF repeats, and non-specific binding of primers to similar regions. The original degenerate fragment, the 5′ RACE fragment and several shorter fragments were all used as templates for probes for in situ hybridization. All of these fragments gave an identical expression pattern.

hunchback

Degenerate primers were used on genomic DNA. The forward primer PFVTEYKHH (CCCTTCGTGACCGAGTACAARCAYCAYYT) and the reverse primer KYCHFSKLH (GCAGCTTGAAGGAGTGGCARTAYTTNGT) gave a 212 bp fragment of *hunchback*. This sequence was extended using inverse PCR, to give 666 bp of coding sequence (GenBank accession AY995117). Specific primers were designed against the ends of this sequence (forward primer CAAGACGTATCGATGCAAGCAG and reverse primer ATTTTCCGTCGCCGCATGAATAAG). The resulting 658 bp PCR product was used as a template for in situ hybridization.

Krüppel

Degenerate primers were designed against conserved zinc finger motifs in *Krüppel* sequences available from GenBank. Positive PCR results were obtained with the forward primer YKHVLQNH/Q(TACAAGCACGTGYTRCARAAYCA) and the reverse primer FSDSNQLK(TTCAGTTGRTTRSWRTCRSWRAA). The resulting 269 bp sequence was extended using inverse PCR, and a specific 368 bp fragment (GenBank accession AY995118) was cloned using the specific primers forward: TTGCAGAATCACGAGCGAACGCAC and reverse: TTCTCGTCCTTCGGGCACTTGTGA. This fragment was used as a template for in situ hybridization experiments.

Histology and stainings

FITC-phalloidin stainings were performed as described previously (Stollewerk, 2000). Embryos were fixed and sectioned for light microscopy as described by Stollewerk et al. (1996).

Results

Development at late- and postsegmentation stages

In order to provide developmental reference points for accurately staging fixed embryos, we devised a staging table based on evident characters that are not related to neural development. Chipman et al. (2004b) described seven embryonic stages in *S. maritima* based on morphological features visible in live embryos. We found that neurogenesis in the trunk takes place mostly during stages 5–6. Our staging system subdivides these stages based on characters that can be seen in fixed and mounted specimens.

Chipman et al. (2004b) described stage 5 as the final stage of the segmentation process. We divided this stage into three substages, based on the number of segments, the number of limb buds, and the degree of differentiation of the anterior segments.

Stage 5a: 30–40 morphologically distinct leg-bearing segments are visible. The posterior undifferentiated area is wider than the germ band and is still slightly rounded. The antennae are flat and are club shaped, with a narrow base and a broad rounded distal end. The 2nd maxilla and the maxilliped are approximately the same length, with the maxilliped slightly wider, and both are the same length as the limb buds of the first leg-bearing segment. Limb buds can be seen in up to 10 leg-bearing segments.

Stage 5b: Over 40 leg-bearing segments are visible. The size of the posterior undifferentiated region has reduced to the width of the germ band. The 2nd maxilla is slightly longer than the maxilliped. Limb buds can be seen in half of the leg-bearing segments.

Stage 5c: The full complement of segments is visible. The proctodeum starts migrating posteriorly. The 2nd maxilla develops a small pointed distal extension. The base of the antennae starts broadening. The maxilliped is longer than the limb bud of the first leg-bearing segments. Limb buds can be seen in more than half of the leg-bearing segments.

At stage 6, the germ band splits along the midline, and the two halves begin to migrate laterally (Chipman et al., 2004b). During lateral migration, the embryo bends inward and the middle part of the trunk region begins folding into the yolk. This process continues until the entire germ band has sunk into the yolk, ventral side facing inwards, and the embryo lies with the anterior and posterior ends juxtaposed. The end of germ band sinking defines the end of stage 6 (Chipman et al., 2004b). We divided this stage into three substages.

Stage 6a: The lateral margins of the germ band separate. The proctodeum is at a posterior position and opens posteriorly, with a clearly visible hindgut extending anterior from the opening. The bases of the antennae are broad and the antennae are cone shaped. The 2nd maxilla has a distinct narrow distal portion. The maxilliped is approximately 50% wider and somewhat longer than the limb bud of the first leg-bearing segment. Limb buds can be seen in all but the posterior 2–3 leg-bearing segments.

Stage 6b: The lateral margins of the germ band have separated noticeably and the central portion starts sinking into the yolk. The 1st maxilla has extended and is twice as long as it is broad. The maxillipeds are approximately 50% wider and 50% longer than the limb buds of the first leg-bearing segment. Limb buds can be seen on all leg-bearing segments.

Stage 6c: The germ band has partly sunk into the yolk and is folded on itself. The hindgut has extended almost up to the most posterior leg-bearing segments. The width of the antennae has increased and they are cone shaped. The distal portion of 2nd maxilla is curved anteriorly. The maxillae have increased substantially in size and have developed a secondary medial lobe.

Morphology of neural precursor formation in S. maritima

As the segments arise from the posterior undifferentiated disc in *S. maritima*, they are broad along the medio-lateral axis, and anterio-posteriorly compressed (Figs. 1A, B). Shortly after their first appearance, they become separated into left and right hemi-segments by ventral midline cells. In order to analyze neurogenesis in *S. maritima*, we stained embryos with phalloidin-FITC, a dye that stains the actin cytoskeleton. Because the actin filaments stained by this agent are mainly found in the cortex of the cell, this technique can be used to investigate the morphology of the neuroectodermal cells in the confocal laser-

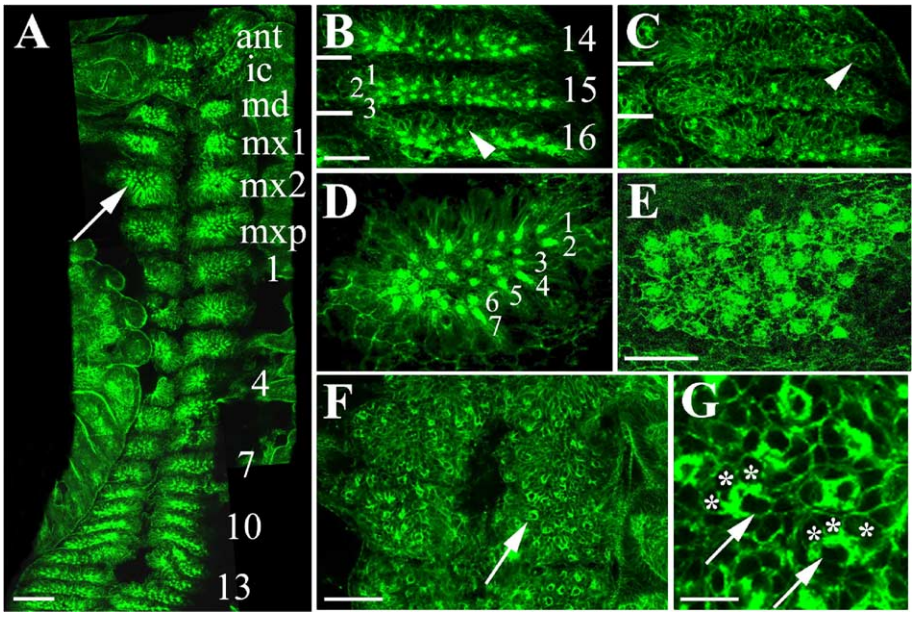

Fig. 1. (A–G) Morphology of neural precursor formation in *S. maritima.* Confocal micrographs of flat preparations of embryos at stage 5a stained with phalloidin-FITC; anterior is towards the top, the midline towards the left. (A) The dot-like phalloidin staining corresponds to the constricted cell processes of the neural precursor groups (arrow). (B) In the posterior part of the germ band, the neural precursor groups are arranged in three rows per hemi-segment (arrowhead). The white lines indicate the segmental borders. (C) Basal optical section of the same hemi-segment shown in panel B. Groups of basally enlarged cells are located underneath the dots of high phalloidin staining (arrowhead). (D) Cell movements lead to a rearrangement of the invagination sites. In the anterior region of the germ band, invagination sites are arranged in 7 rows per hemi-segment with 3 to 6 invagination sites each. The pattern is comparable to the spider and the other myriapods. (E) Pattern of invagination sites in a hemi-segment of *G. marginata* corresponding to the second leg (for details see Dove and Stollewerk, 2003). (F) Optical section 2 μm basal to the spot-like phalloidin staining. Phalloidin accumulates around single cells (arrow). (G) Higher magnification of neural precursor groups in the same plane shown in panel F. The cell processes of the neural precursors (asterisks) are attached to a single cell of the precursor group (arrows). ant, antennal segment; ic, intercalary segment; md, mandibular segment; mx1 to 2, 1st and 2nd maxillary segment; mxp, maxilliped; 1 to 16, leg-bearing segments 1 to 16. Scale bars: 80 μm in panel A, 30 μm in panels B–D, 10 μm in panel E, 60 μm in panel F, 30 μm in panel G.

scanning microscope (LSM). At stage 5a, neurogenesis is initiated about 5–6 segments anterior to the last visible segmental furrow (referred to hereafter as segment P). Similar to the spider and both myriapods that have previously been analyzed (Stollewerk et al., 2001; Dove and Stollewerk, 2003; Kadner and Stollewerk, 2004), we detected dots of high phalloidin staining in apical optical sections of the neuroectoderm (Figs. 1A, B, D). LSM analysis of serial Z-sections revealed that the constricted cytoplasmic processes of invaginating neural precursor groups correspond to the spot-like phalloidin staining in the apical region of the neuroectoderm (Fig. 1C). Similar to the diplopod *G. marginata*, we counted up to 12 cells per invagination site (Dove and Stollewerk, 2003), while in the spider, *C. salei* and in the chilopod *L. forficatus* 5 to 9 cells form one invaginating cell group. As in the spider and in the other myriapods analyzed, about 30 invaginating cell groups are generated per hemi-segment in *S. maritima* (Figs. 1B, D). All invagination sites are already present in narrow posterior segments at stage 5a. However, in contrast to the other species analyzed, they are arranged in 3 rows per hemi-segment with 7 to 12 invagination sites each (Fig. 1B). Interestingly, the morphogenetic movements that reduce the medio-lateral extent of the neurogenic domain lead to an arrangement of the invagination sites that is similar to the other myriapods and the spider: in the anterior region of the germ band, they are arranged in 7 rows per hemi-segment with 3 to 6 invagination sites each (Fig. 1D, compare to *G. marginata* Fig. 1E).

Further analyses of the morphology of the invagination groups revealed a striking difference to the spider and the other myriapods. In *S. maritima*, the cell processes of the neural precursors are not attached to the apical surface but to a single cell of the precursor group (Figs. 1F, G).

During stage 6a, all the cells of the neural precursor groups detach from each other in an anterior to posterior gradient beginning in the head segments. Interestingly, the longitudinal axon tracts are already visible along the entire trunk at stage 5b before the neural precursors detach from each other in the head and trunk segments (Fig. 2A, arrow). These data suggest that the longitudinal axon tracts are formed by axonal projections of neurons located in the cephalic lobe. Alternatively, individual neural precursors might have already detached from the precursor groups and pioneered the longitudinal axon fascicles.

It has been shown in *C. salei* and *G. marginata* that the central region of the ventral neuroectoderm gives rise exclusively to neural precursors. The epidermis arises lateral and medial to the neuroectoderm and overgrows the neuromeres during or shortly after invagination of the neural precursors. Similar to *G. marginata*, the central area of the neuroectoderm of *S. maritima* sinks into the embryo and the epidermis overgrows the neuromeres (Fig. 2B, arrow).

The neurogenic genes Notch and Delta are expressed during neural precursors formation

To see whether the genetic network that leads to the specification of neural precursors is conserved in *S. maritima*, we cloned *Notch* and *Delta* homologues. We have identified one *Delta* and one *Notch* homologue. The *Delta* sequence of *S. maritima* is most similar to that of the previously studied centipede *L. forficatus* and to the millipede *G. marginata* (64% and 57% identity at the amino acid level, respectively—with a unique insert of 4–5 amino acids in *G. marginata*), and shows roughly the same similarity to *C. salei* and *D. melanogaster* (53% and 54% identity, respectively). Due to the limitations of the PCR-cloning technique, we cannot rule out the possibility of two *Delta* orthologues in the genome (as found in *C. salei*). The *S. maritima Notch* sequence was obtained by initial PCR with degenerate primers and 5′ rapid amplification of cDNA ends (RACE). It aligns unambiguously with the expected EGF repeats 12–19 of *D. melanogaster* and shows the highest similarity to the *D. melanogaster* sequence at the amino acid level (68% identical amino acids).

S. maritima Delta shows a dynamic expression pattern in the ventral neuroectoderm during the whole course of neurogenesis. *Delta* expression is first visible at mid-stage 3 in groups of cells in the first three head segments. At this stage, five out of six head segments can be distinguished morphologically. After 25 segments have been formed (stage 4), *Delta* is expressed in additional cell groups in the head segments and the expression has extended up to segment 22 (data not shown). Since the whole dynamic of *Delta* expression is visible at stage 5, we analyzed this stage in detail. At stage 5a, *StmDelta* is expressed in a single group of neural precursors in the most posterior hemi-segment of the embryo that exhibits neurogenesis

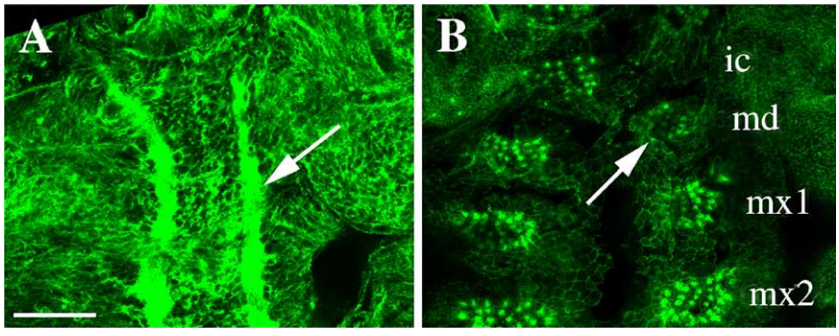

Fig. 2. (A–B) Late neurogenesis in *S. maritima*. Confocal micrographs of flat preparations of embryos stained with phalloidin-FITC; anterior is towards the top. (A) Basal optical section showing axon tracts in a stage 5b embryo (arrow). (B) The epidermis overgrows the ventral neuromeres after formation of all invagination sites (arrow). ic, intercalary segment; md, mandibular segment; mx1 to 2, 1st and 2nd maxillary segment. Scale bar: 80 μm in panels A–B.

(representing the earliest stage of neurogenesis) (Fig. 3A). This segment is approximately 5 segments anterior to segment P, and is referred to as P-5. In the next anterior (developmentally older) hemi-segment, *Delta* transcripts accumulate in an additional cell group. The same pattern is visible in the following segment. In progressively more anterior segments, more and more neural precursor groups start expressing *StmDelta* with no more than four hemi-segments showing the same expression pattern at the same time (Fig. 3A). A comparison of the same region of the germ band in an older embryo (stage 5b) reveals that additional neural precursor groups arise first medially and then in between the existing cell groups (Fig. 3B). In addition, the gene is expressed in a number of cells in the lateral germ band and limb buds, which we interpret as belonging to the developing peripheral nervous system (Fig. 3B, large arrowhead). *StmDelta* seems to be expressed at higher levels in single cells of the precursor groups (Figs. 3C, D, arrows). Alternatively, *Delta* transcripts might accumulate around individual cells, since the cell processes of all cells of an invagination group are attached to a single cell of the group (see above). Due to the peak and trough-like structure of the segments, invaginating cell groups occupy different dorso-ventral positions in the neuroectoderm (Fig. 3D, arrows).

S. maritima Notch is expressed ubiquitously throughout neural development. In the cephalic lobe and in the ventral neuroectoderm, *Notch* transcripts accumulate in single cell groups (Figs. 4A, C, D). Similar to the spider *CsNotch*, *StmNotch* is transiently expressed at higher levels in the lateral region of the ventral neuroectoderm facing the limb buds (Figs. 4B, E, arrows). In addition, *StmNotch* transcripts can be detected in the ventral midline (Fig. 4B, arrowhead).

To summarize, Strigamia *Delta* and *Notch* genes are expressed during neurogenesis indicating that they might play a role in neural precursor specification similar to the chelicerate and the other myriapods analyzed.

Specification of neural precursor identity in S. maritima

In order to analyze whether homologues of *Drosophila* neural identity genes might generate diversity among neural

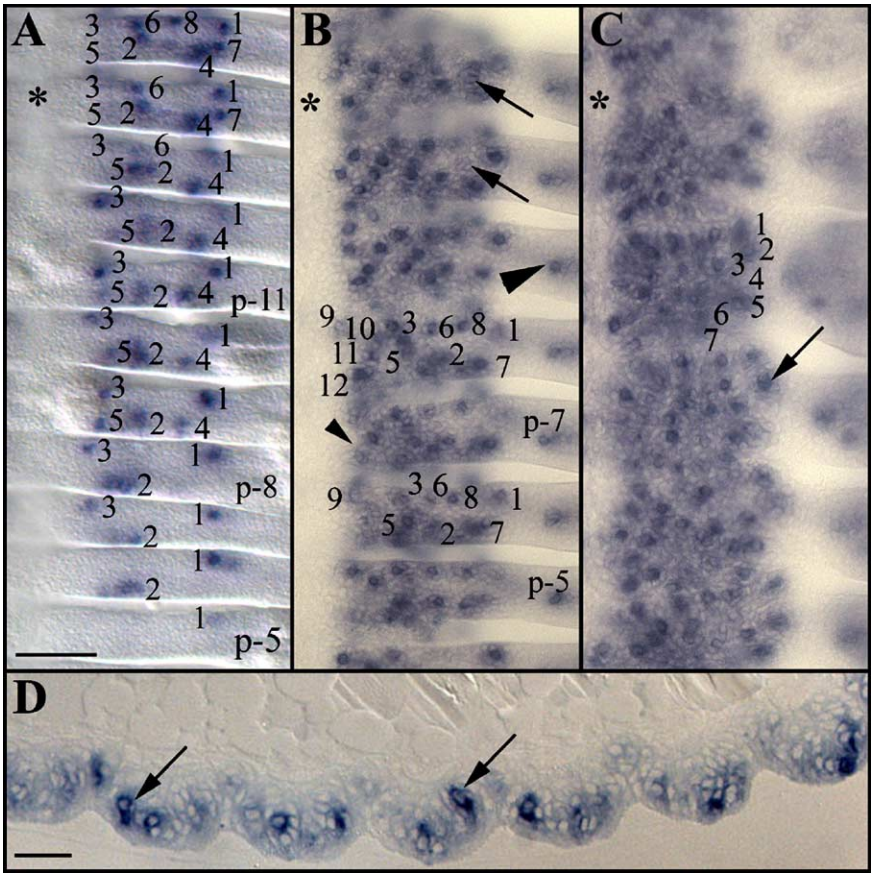

Fig. 3. (A–D) Expression pattern of *S. maritima Delta* in the ventral neuroectoderm. Light micrographs of flat preparations (A–C) and sagittal section (D) of embryos stained for a DIG-labeled *StmDelta* probe; anterior is towards the top, the midline towards the left in panels A–C, anterior is towards the left in panel D. (A) Sequential expression of *StmDelta* in the most posterior segments that undergo neurogenesis in a stage 5a embryo. The neural precursor groups are numbered 1 to 8 in order of appearance. The asterisk marks the midline. See text for further explanation. (B) Pattern of *StmDelta* expression in neural precursor groups in the same region of the germ band shown in panel A in a stage 5b embryo. Additional neural precursor groups arise first medially (small arrowhead) and then in between the existing cell groups (arrow). In addition, the gene is expressed in the developing peripheral nervous system (large arrowhead). (C) In the anterior region of the germ band, all 30 neural precursor groups are present. They are arranged in 7 rows. *StmDelta* transcripts accumulate either in cell processes around single cells or in single cells (arrow). Note that not all groups are visible because they are in different focal planes (see below). (D) Due to the peak and trough-like shape of the segments, the precursor groups are located in different focal planes (arrows). 80 μm in panels A–C, 40 μm in panel D.

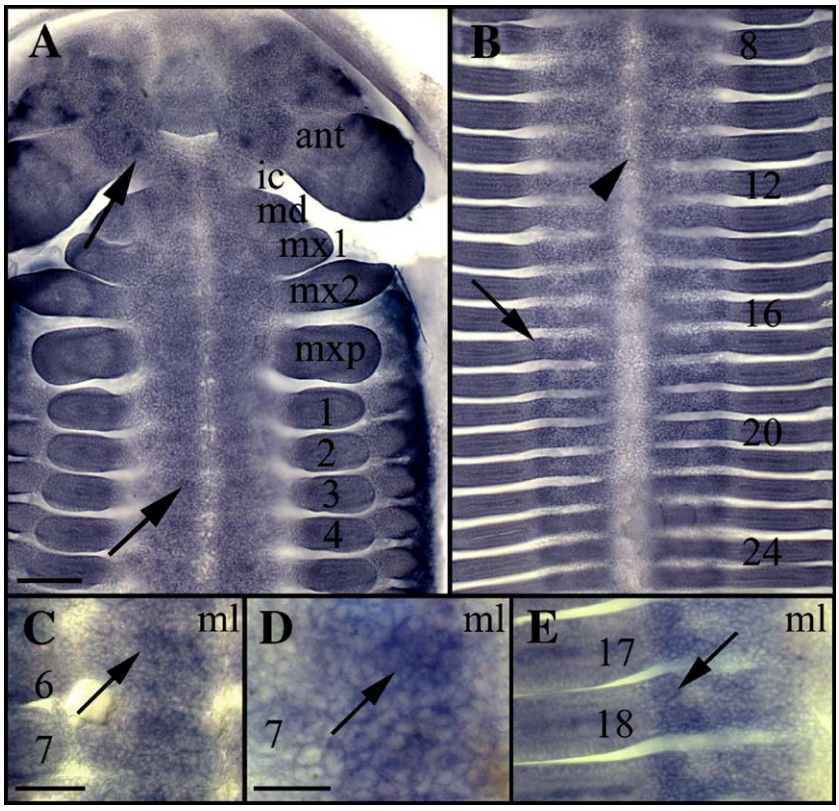

Fig. 4. (A–E) Expression pattern of *StmNotch* during neurogenesis. Light micrographs of flat preparations of embryos stained for a DIG-labeled *StmNotch* probe; anterior is towards the top. (A) At stage 5b, *StmNotch* is expressed ubiquitously in the germ band. In the cephalic lobe and in the ventral neuroectoderm, *Notch* transcripts accumulate at higher levels in single cell groups (arrows). (B) *StmNotch* shows a transient stronger expression in the lateral area of the neuroectoderm facing the limb buds (arrow). In addition, the gene is expressed in the ventral midline (arrowhead). (C, D) Higher magnification of two hemi-segments (C) and one hemi-segment (D), respectively, showing accumulation of *Notch* transcripts in cell groups (arrows). (E) Higher magnification of three hemi-segments. *Notch* is transiently expressed at higher levels in the lateral region of the ventral neuroectoderm (arrow). ant, antennal segment; ic, intercalary segment; md, mandibular segment; mx1 to 2, 1st and 2nd maxillary segment; mxp, maxilliped; 1 to 24, leg-bearing segments 1 to 24; ml, ventral midline. Scale bars: 120 μm in panels A–B, 80 μm in panels C, E, 40 μm in panel D.

precursors despite the differences in formation, we cloned *hunchback* and *Krüppel* in *S. maritima* and examined their expression during neural development.

The 666 bp of coding sequence recovered from the *S. maritima hunchback* homologue encodes four C2H2 zinc-finger domains that align with insect *hunchback* sequences with a high degree of conservation (69% identity with *D. melanogaster* for the first 116 amino acids). This is followed by a stretch 80 amino acids with no obvious homologies, and finally, an additional C2H2 domain that does not match any of the insect *hunchback* domains, although a terminal C2H2 domain is present both in insects and in *Caenorhabditis elegans*. There are no published sequences for *hunchback* in other myriapods or in chelicerates, so we cannot yet determine how specific these divergent domains are.

The 368 bp *Krüppel* sequence encodes just over four C2H2 zinc-finger domains. These domains align with the *D. melanogaster* sequence, and with a series of short fragments cloned from a variety of arthropods (Sommer et al., 1992). The first 115 amino acids match the *Drosophila* sequence with 85% identity. The short (46 aa) sequence available for the centipede *L. forficatus* shows 89% identity to the *S. maritima* sequence.

The expression pattern of *hunchback* during neurogenesis can be subdivided into several phases. *hunchback* is expressed in the whole neuroectoderm of the first three head segments at about the same time (stage 3) as the first neural precursor groups express *Delta* in the same region. This expression pattern extends up to segment 22 at the 25 segment stage, and covers the same domain where *Delta* is expressed. While a strong expression of *hunchback* is maintained in the anterior region of the germ band up to the first maxillary segment, *hunchback* is down-regulated in the second maxillary segment and the maxilliped. In several segments posterior to the maxilliped, *hunchback* transcripts accumulate in groups of cells (data not shown).

Since all phases of expression are visible in stage 5 embryos, due to the anterior–posterior gradient of development, we compared *hunchback* expression with the distribution of *StmDelta* transcripts at the same stage to visualize the progression of neurogenesis during the different phases (Fig. 5, see also Fig. 7H). At stage 5c, the full complement of segments is visible. Since the number of segments is variable in *S. maritima*, we compared *Delta* and *hunchback* expression in all specimens by numbering the segments from the posterior most segment (segment P). *hunchback* is expressed in the whole neurogenic region of the 10 most posterior (developmentally youngest) segments (Figs. 5B, C, arrows). In this region, the first neural precursor groups have been gradually specified,

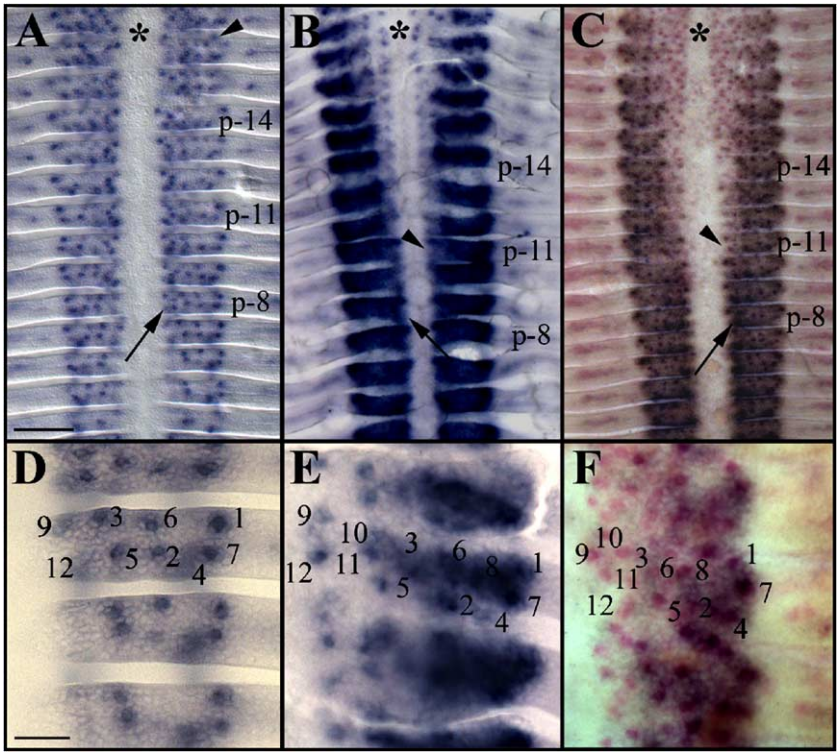

Fig. 5. (A–F) Expression of *hunchback* and *Delta* during neural precursor formation. Light micrographs of flat preparations of stage 5c embryos single-stained for a DIG-labeled *StmDelta* probe (A, D) and a DIG-labeled *Stmhunchback* probe (B, E), and double-stained for *Stmhunchback* (DIG) and *StmDelta* (Fluorescein) (C, F); anterior is towards the top. The asterisks indicate the ventral midline. (A) Neural precursors are formed sequentially. The arrow points to the area in which neural precursors 9 to 12 are forming. Additional precursor groups (arrowheads) are generated after restriction of *hunchback* to the first 12 precursor groups. (B) Three phases of *hunchback* expression are visible. In the most posterior region of the germ band, *hunchback* is expressed in the whole ventral neuroectoderm, although there is a weaker expression close to the midline (arrow). Further anterior *hunchback* expression decreases in the medial third of the segments (arrowhead). In the following anterior segments, hunchback transcripts become restricted to groups of cells and single cells. (C) *StmDelta* (red) and *hunchback* (brown) double-labeling shows that *hunchback* covers the area in which precursor groups 1 to 12 arise. The arrowhead points to the medial domain where *hunchback* is down-regulated. (D) At higher magnification, *Delta* staining reveals the arrangement of the first 12 precursor groups. Note that not all groups are visible because they are not in the same focal plane due to the specific morphology of the segments. (E–F) *hunchback* expression is restricted to the first 12 precursor groups. Note that the precursor groups in panels E and F are not exactly in the same position due to the morphogenetic movements that lead to elongation of the germ band. p-8 to p-14, 8th to 14th posterior segment. Scale bars: 120 μm in panels A–C, 40 μm in panels D–E.

with one invagination group being visible in hemi-segment P-3 and 12 in hemi-segment P-8 (Fig. 5A). In segment P-11, *hunchback* expression decreases in the medial region of the hemi-segments (Figs. 5B, C, arrowheads). The same expression pattern is visible in the next following hemi-segments up to segment P-14. This area covers the region where neural precursor groups 9 to 12 are forming at this time (Figs. 5A, C, arrows). There is an overlap of low level expression of *hunchback* and up-regulation of *Delta* transcripts in the medial area. *hunchback* expression then becomes restricted to the 8 first-generated groups of neural precursors in the lateral region of the neuroectoderm and to precursor groups 9 to 12 in the medial region. Additional precursor groups do not arise until the restriction of *hunchback* expression to the 12 first-generated precursor groups (Fig. 5A, arrowhead).

hunchback expression in the neuroectoderm decreases in further anterior segments (Figs. 5B, C and 6A, arrowhead). However, in this area, *hunchback* is expressed in about 20 cells that are located basally (Figs. 6B, C). The expression is first visible in a transverse row of cells and a few cells located close to the ventral midline (Fig. 6B). In further anterior (developmentally older) segments, *hunchback* transcripts accumulate in a group of basal cells in the medial region of the neuromeres. Since the number of *hunchback* positive cells remains the same, we assume that the scattered *hunchback* expressing cells migrate to a medial position and are therefore identical to the medial cell group. However, this has to be confirmed by single cell labeling. Based on the position of these cells and the fact that neural precursors have already invaginated during this time, we assume that this pattern corresponds to a neuronal expression of *hunchback*.

hunchback is strongly expressed in the cephalic lobe and in all invagination groups in the antennal, intercalary, and mandibular segments throughout neurogenesis. In addition, *hunchback* is expressed in the mesoderm. The mesodermal expression is already visible in the undifferentiated posterior area of the germband (Fig. 6D, arrowhead). A stronger expression is seen in the most anterior region of the blastodisc where the youngest segment is forming. In this area, *hunchback* is expressed in a patchy transverse stripe (Fig. 7B, leg-bearing segment 43). Interestingly, a similar expression pattern has been observed in the insects *Schistocerca americana*, *Musca domestica*, and *Tribolium castaneum* (Sommer and Tautz, 1991; Wolff et al., 1995; Patel et al., 2001). The

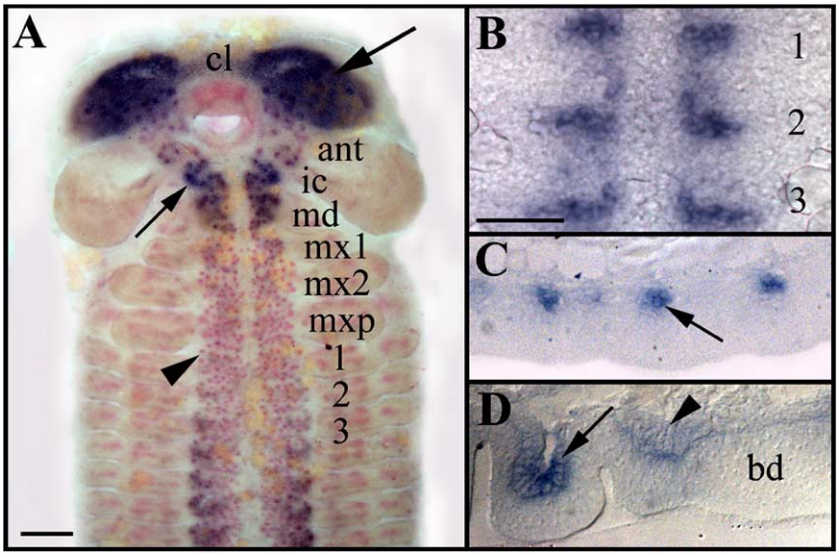

Fig. 6. (A–D) *hunchback* expression during late neurogenesis. Light micrographs of flat preparations (A, B) and sagittal sections (C, D) of embryos double-stained for a Fluorescein-labeled *StmDelta* probe and a DIG-labeled *Stmhunchback* probe (A) and single-stained for *Stmhunchback* (B–D); anterior is towards the top in panels A and B and to the left in panels C and D. (A) *hunchback* expression (blue) in the neuroectoderm decreases in the anterior segments of the germ band (arrowhead). *hunchback* is strongly expressed in the cephalic lobe and in all invagination groups in the antennal, intercalary, and mandibular segments throughout neurogenesis (arrows). (B) In the basal area of the posterior head segments (not shown) and in the first three trunk segments, *hunchback* is expressed in about 20 neurons. Expression appears first in a transverse row of cells. In further anterior (developmentally older) segments, *hunchback* is expressed in a group of cells close to the ventral midline. (C) This cell group is located in the most basal region of the ventral neuromeres (arrow). (D) In addition, *hunchback* is expressed in the mesoderm (arrow). Expression is first visible in the anterior region of the undifferentiated posterior area (arrowhead). ant, antennal segment; cl, cephalic lobe; ic, intercalary segment; md, mandibular segment; mx1 to 2, 1st and 2nd maxillary segment; mxp, maxilliped; 1 to 3, leg-bearing segments 1 to 3. Scale bars: 160 μm in panel A, 80 μm in panels B–D.

striped appearance is probably due to a compaction of the mesoderm during morphological segmentation (Patel et al., 2001). In contrast, in *Drosophila*, *hunchback* is only expressed later during development in specific mesodermal cells that are involved in tracheal guidance (Wolf and Schuh, 2000).

Similar to *hunchback*, *S. maritima Krüppel* expression is first visible in the head segments at stage 3, in a restricted medial region of each head segment and the maxillipede (data not shown). However, *Krüppel* transcripts continue to be detected later than *hunchback*. At stage 4, *Krüppel* transcripts accumulate in the whole neurogenic region of the head segments and the maxillipede, while expression can now be detected in restricted medial regions in leg-bearing segments 1 to 7 (Fig. 7A). To analyze spatial and temporal differences in the expression pattern, we compared *hunchback* and *Krüppel* expression in embryos of the same stage. Because of the high level of expression of *Krüppel*, and its wide expression domain, we were technically unable to do double staining for *Krüppel* and *hunchback* together. However, by comparing the expression of the two genes at the same axial level in embryos of the same stage (based on the morphological staging scheme described above), we were able to correlate their expression domains and determine where they overlap and where they are mutually exclusive. At stage 5b, *Krüppel* is absent from the medial region of the posteriormost 3–4 segments. It is expressed at low levels in the medial region of segments P-4 to P-10 (Fig. 7B). Since the first invagination sites arise lateral in the neuroectoderm (see Fig. 3A), the expression domain does not cover the area where neural precursors are specified at this time. In segments P-3 to P-8, *Krüppel* expression gradually increases in the medial domain and extends laterally. A comparison with *hunchback* expression in embryos of the same stage suggests that *Krüppel* is expressed in the medial region where *hunchback* expression decreases in developmentally older segments (Figs. 7B, C, arrowhead; Figs. 7G, H). Further anterior and in older embryos, *Krüppel* transcripts accumulate in the whole neurogenic region (Figs. 7D, G, I). In addition, the gene is expressed in the ventral midline and in the developing limb buds (Fig. 7D). In this area in comparable embryos, *hunchback* expression has already been switched off in the neuroectoderm, and transcripts can be detected in basally located cells (Figs. 7D, inset, G, H). In older segments, *Krüppel* expression accumulates in the lateral region of the neuroectoderm (Figs. 7D, E, I). Subsequently, expression is first reduced in the medial regions of the neuroectoderm and then in the lateral domain (Figs. 7E, I). *Krüppel* is expressed at low levels in the basal neuronal cell layers (Fig. 7F).

Discussion

Distinct mode of neurogenesis in S. maritima

Similar to the chelicerates and other myriapods analyzed, about 30 groups of neural precursor cells are specified in each hemi-segment, and invaginate from the ventral neuroectoderm of the geophilomorph centipede *S. maritima*. However, *S. maritima* neurogenesis shows several distinct features that cannot be found in the other species studied. (1) The morphology of the invagination sites is different in *S. maritima*. In the spider and the other myriapods, the constricted cell processes of the neural precursor groups

extend to the apical surface of the neuroectoderm. In contrast, in *S. maritima*, the cell processes of the neural precursors are not attached to the apical surface but to a single cell of the precursor group. We speculate that this specific morphology is necessary for the rearrangement of the neural precursor groups during the medio-lateral intercalation movements that lead to the final pattern of invagination sites in 7 rows. Since all cells of a precursor group are attached to a single cell of the group, they can be moved together during this process. In contrast, in the spider and the other myriapods, the arrangement of the invagination sites remains the same throughout neurogenesis. (2) In *S. maritima*, neural precursor groups are specified one-by-one at stereotyped positions in the ventral neuroectoderm. In contrast, in the spider and the other myriapod species, neural precursor groups are generated in several waves with 5 to 8 precursor groups arising per wave. The different mode of neural precursor formation in the centipede *S. maritima* might be an adaptation to the distinct embryonic development of this species. About 50 segments are generated during embryogenesis and differentiate in quick succession. Our expression studies and morphological analyses have revealed that each segment exhibits a different differentiation state along the anterior–posterior axis during neurogenesis. Therefore, we conclude that each segment initiates neurogenesis on its own, rather than being synchronized with several segments as seen in the spider and in the other myriapods. (3) In *S. maritima*, neural precursor groups are initially arranged in 3 rows. However, similar to the other species analyzed, the invagination sites arise at stereotyped positions indicating that the identity of the neural precursors depends on their accurate position in the ventral neuroectoderm. It can be assumed that the transition from 3 to 7 rows of invagination sites is based on convergent extension movements. During this process, cells elongate, align, and then intercalate, generating longitudinal germ band extension from latitudinal cell migration. Convergent extension movements seem to follow a predictable pattern since they can be simulated by computer models (Zajac et al., 2003). Accordingly, the final arrangement of invagination sites after medio-lateral intercalation is the same in each hemi-segment suggesting that individual invagination sites are shifted to the same relative position. Future analysis will show if the rearrangement of the invagination sites has an impact on neural precursor identity.

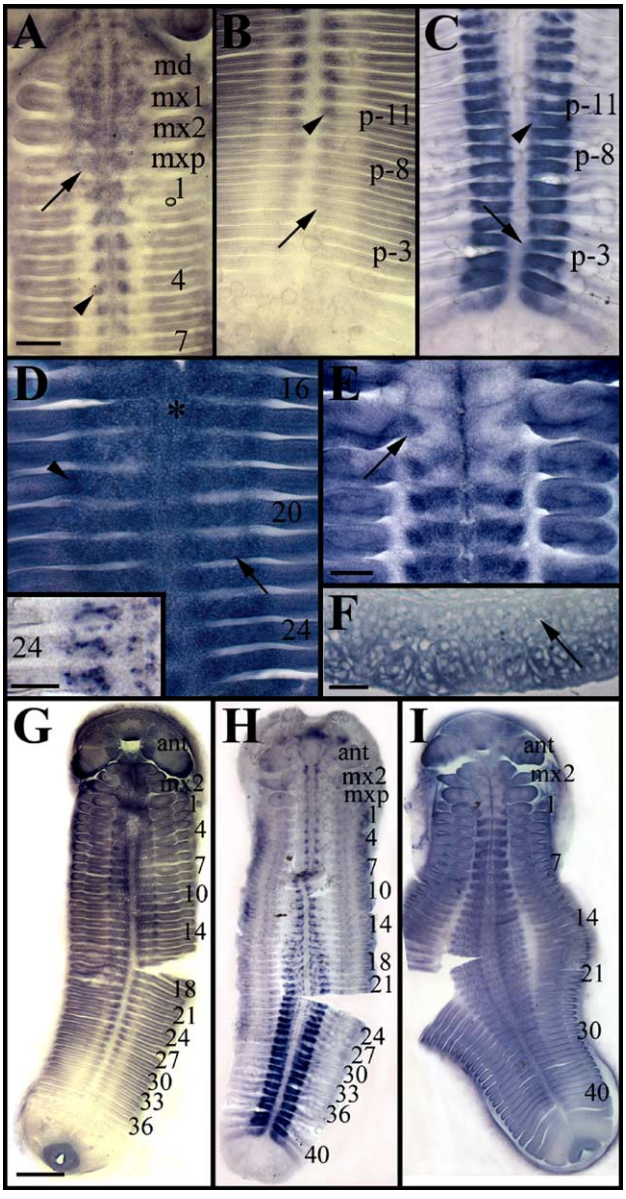

Fig. 7. (A–I) Comparison of *StmKrüppel* and *Stmhunchback* expression during neural precursor formation. Light micrographs of flat preparations (A–E, G–I) and a sagittal section (F) of embryos stained for a DIG-labeled *StmKrüppel* probe and a DIG-labeled *hunchback* probe (C, H); anterior is towards the top in panels A–E and towards the left in panel F. (A) At stage 4, Krüppel is expressed in the whole neurogenic region of the head segments and the maxilliped (arrow). Expression in restricted medial domains is visible in leg-bearing segments 1 to 7 (arrowhead). (B) At stage 5b, *Krüppel* is expressed in a small longitudinal stripe close to the midline in the posterior most segments where expression is visible (arrow). Expression is up-regulated and extends laterally in further anterior segments (arrowhead). (C) *hunchback* is expressed earlier than *Krüppel*. The expression domain covers the whole neuroectoderm but transcripts accumulate at lower levels close to the midline (arrow). In further anterior segments, *hunchback* expression decreases (arrowhead). (D) *Krüppel* transcripts extend laterally and cover the whole ventral neuroectoderm (arrow). In a comparable part of the germ band, *hunchback* has been down-regulated in the neuroectoderm and is now expressed in groups of cells and single cells in basal cell layers (inset). There is a stronger expression in the lateral region facing the limb buds (arrowhead). In addition, *Krüppel* is expressed in the ventral midline (asterisk). (E) At stage 6a, *Krüppel* expression is down-regulated in the head segments and the maxilliped. Expression decreases first in the medial area and then in the lateral domain (arrow). (F) *Krüppel* is not expressed in the basal layers of the neuromeres (arrow). (G) A flat preparation of an embryo at late stage 5a shows *Krüppel* expression in restricted medial domains in the posterior region of the germband and expression in the whole neurogenic region in the anterior part of the embryo. (H) Dynamic expression of *hunchback* during neural precursor formation at about the same stage (early 5b). (I) At stage 6a, Krüppel is expressed in the whole ventral neuroectoderm of the trunk. Expression has decreased in the head segments and in the maxilliped. ant, antennal segment; md, mandibular segment; mx1 to 2, 1st and 2nd maxillary segment; mxp, maxilliped; 1 to 40, leg-bearing segments 1 to 40; p-3 to p-11, 3rd to 11th posterior segment. Scale bars: 120 μm in panels A–C, 80 μm in panels D–E, 40 μm in panel F, 350 μm in panels G–I.

The genetic network leading to neural precursor specification seems to be conserved in S. maritima

According to current models, proneural gene expression is higher in one cell of the proneural cluster due to predetermination or to an extrinsic signal. This leads to an up-regulation of *Delta* in this cell, since the proneural genes activate the expression of *Delta.* Delta activates Notch in the neighboring cells which eventually leads to a repression of proneural gene expression and a down-regulation of *Delta* in neighboring cells (Nakao and Campos-Ortega, 1996; Ligoxygakis et al., 1998). This feedback loop maintains proneural gene expression in the neuroblast but down-regulates it in the remaining cells of the proneural cluster. Similar to *Drosophila*, *Delta* transcripts can be detected in all neuroectodermal cells but accumulate at higher levels in groups of neural precursors in *C. salei*, *G. marginata*, and *L. forficatus* (Stollewerk, 2002; Dove and Stollewerk, 2003; Kadner and Stollewerk, 2004). One *Delta* gene each has been identified in *L. forficatus* and *G. marginata*, while the spider *C. salei* has two *Delta* genes. The spider *CsDelta1* gene is exclusively expressed in the neural precursor groups. In contrast, *CsDelta2* is expressed in all neuroectodermal cells but shows a higher expression in the precursor groups. Similar to *CsDelta1*, *S. maritima Delta* expression is restricted to the neural precursor groups. This expression pattern suggests that neural precursor groups are not singled out from a field of equivalent cells; rather, the position of the precursor group is predetermined by other factors. However, there are two other explanations for the observed expression pattern. (1) *Delta* expression in the remaining neuroectodermal cells is too low to be detected by in situ hybridization. (2) Similar to the spider *C. salei*, a second *Delta* gene is expressed at low levels in the whole ventral neuroectoderm but up-regulated in the neural precursor groups.

The higher accumulation of *StmDelta* transcripts within a single cell or around a single cell of a precursor group suggests that individual cells of the precursor groups are distinct. This assumption is supported by morphological analysis showing that all cells of a precursor group attach to a single cell of the group. Thus, although the whole precursor group will eventually invaginate and give rise to neural cells, Delta/Notch signaling might generate single cells with distinct properties within the precursor groups. These cells might have an important role during convergent extension movements in keeping individual cell groups together (see above).

Specification of neural precursor identity in S. maritima

Our analysis of the expression pattern of *hunchback* and *Krüppel* during neurogenesis raises the possibility that these genes confer temporal identity to neural precursors in the ventral neuroectoderm of *S. maritima*, in a fashion similar to that demonstrated in *Drosophila* (Isshiki et al., 2001). In what follows, we interpret our expression results with this model in mind, although we cannot rule out the possibility that the expression patterns we see reflect a role of *hunchback* and *Krüppel* in neural precursor differentiation after establishment of neural identity.

hunchback shows several distinct phases of expression that can be correlated with a function in early-generated neural precursor groups (Fig. 8). Initially, *hunchback* is expressed in all cells of the ventral neuroectoderm before and during formation of the first 12 neural precursor groups, although there is a weaker expression of *hunchback* in the area close to the midline. Additional precursor groups do not form until restriction of *hunchback* expression to the 12 first-generated groups. If *S. maritima hunchback* functions as a temporal identity gene similar to *Drosophila*, it can only do so *after* specification of neural precursors. Thus, we can assume that the gene is specifically required in the 12 first-generated precursor groups, although it is initially expressed in the whole neuroectoderm. After down-regulation of *hunchback* expression in the ventral neuroectoderm, transcripts can be detected in about 20 neurons that are ultimately located in a medial position in the deepest layer of the neuromeres. The fact that each invagination group consists of up to 12 cells suggests that *hunchback* expression is only maintained in a subset of neurons that arise from the 12 first-generated precursor groups. Furthermore, since all invagination sites are still visible at this time, we suggest that single cells of an invagination group detach from the remaining neural precursors, delaminate, and

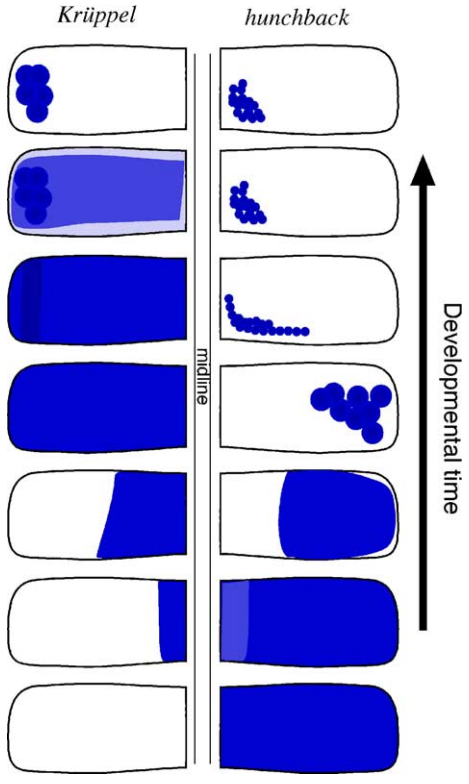

Fig. 8. Schematic representation of the dynamic expression patterns of *hunchback* (right) and *Krüppel* (left). For each time point, two equivalent hemi-segments are presented in mirror image on opposite sides of the midline, each one showing the expression of one of the two genes. Darker shades of blue represent a higher level of expression. The patterns shown span the entire duration of the events we followed, and in reality would not all be seen in a single embryo. See text for detailed explanation of the expression patterns.

start to differentiate. This is an important finding, since it suggests that *hunchback* is not only differentially expressed in individual groups but also within the precursors of a group.

Similar to *hunchback*, *Krüppel* expression can be subdivided into several phases (Fig. 8). *Krüppel* is expressed later than *hunchback* and transcripts first accumulate at low levels in the medial *hunchback* domain that shows a lower expression. When *hunchback* expression decreases in the medial third of the segments, *Krüppel* expression is up-regulated and extends laterally into this domain. During this time, precursor groups 9 to 12 are formed in this area. Assuming a *Drosophila*-like model, this suggests that both *Krüppel* and *hunchback* might specify neural precursor identity in these groups. After down-regulation of *hunchback* in the ventral neuroectoderm, *Krüppel* transcripts cover the area in which neural precursor groups 12 to 30 arise, suggesting that the gene might be involved in specification of neural precursor identity in these groups. The up-regulation of *Krüppel* expression in some groups in the lateral areas of the segments suggests a distinct role for *Krüppel* in these precursors. However, future analysis will show if Pdm and Castor generate additional diversity among the *Krüppel* positive precursor groups, similar to *Drosophila*.

Interestingly, it has been shown recently, that in the spider *C. salei Krüppel-1* transcripts cannot be detected in the ventral neuroectoderm until formation of the third wave of neural precursors indicating that both in *C. salei* and in *S. maritima*, *Krüppel* is expressed in middle-born neural precursors (Stollewerk et al., 2003). At this time, *CsKrüppel-1* is expressed in almost all neuroectodermal cells in the prosoma, but transcripts accumulate at higher levels in the neural precursor groups. These data suggest that a similar, time-dependent expression of neural identity genes might operate both in chelicerates and myriapods.

In *Drosophila*, neuroblasts and their progeny can be identified based on their position and the expression of molecular marker genes. Using these tools, it has been shown in *Drosophila* that Hunchback and Krüppel are necessary and sufficient to specify temporal fates of early-born and middle-born ganglion mother cells and neurons, respectively (Isshiki et al., 2001; Novotny et al., 2002). Similar to *S. maritima*, an overlap of *hunchback* and *Krüppel* expression in the neural precursors and their early-born progeny has also been observed in *Drosophila*. Unfortunately, molecular markers that distinguish between precursor groups or even individual cells within a precursor group are not yet available in myriapods. Therefore, it was not possible to carry out a functional analysis to test whether *hunchback* and *Krüppel* function is conserved in *S. maritima*. However, the expression data are consistent with a model in which *hunchback* specifies neural precursor identity in the 8 first-generated precursor groups, both *hunchback* and *Krüppel* are required in precursor groups 9 to 12 and in addition, *Krüppel* is involved in specifying neural precursor identity in the remaining groups.

The molecular mechanisms underlying temporal patterning in *Drosophila* are not completely understood. Although regulatory interactions exist among the temporal identity genes, inactivating these transcription factors does not prevent the expression of factors specifying the later part of the lineage. It has been shown recently that the switch from *hunchback* to *Krüppel* expression is regulated transcriptionally and requires neuroblast cytokinesis, while the transition from *Krüppel* to *Pdm* and *Castor* is cell cycle-independent (Grosskortenhaus et al., 2005). In addition, Hiromi and co-workers demonstrated that seven-up is required to switch off *hunchback* at the proper time (Kanai et al., 2005).

A comparison of *hunchback* and *Krüppel* expression in *S. maritima* indicates that *Krüppel* is not expressed within the *hunchback* expression domains that show high levels of transcripts, rather the gene is switched on and up-regulated in areas with low levels of *hunchback* expression (Fig. 8). This expression pattern raises the possibility that *S. maritima* Hunchback represses *Krüppel* at high concentrations, while *Krüppel* expression is permitted or activated at low concentrations. Alternatively, Krüppel might repress *hunchback* expression and *Krüppel* transcription is activated by other factors. Interestingly, a concentration-dependent regulation of *Krüppel* by Hunchback has been shown to be involved in the subdivision of the anterior–posterior axis in *Drosophila* (Hülskamp et al., 1990; Schulz and Tautz, 1994; Wu et al., 2001).

However, we can rule out a function of *S. maritima hunchback* and *Krüppel* in segmentation since the ectodermal expression of these genes is not seen until formation of the segments. Similarly, *hunchback* orthologues of the nematode *C. elegans* and the leech *Helobdella triserialis* are not expressed in an anterior to posterior gradient in the early embryo (Savage and Shankland, 1996; Fay et al., 1999; Iwasa et al., 2000). Taken together, these data suggest that the neural function of *hunchback* is ancestral. An incorporation of *hunchback* into the segmentation cascade did not occur until the emergence of the lineage leading to insects and probably crustaceans, but the regulatory interactions of the genes involved might have already been established in chelicerates and myriapods.

Evolutionary scenario

In vitro and in vivo data suggest that specification of temporal identity depends largely on intrinsic regulation in *Drosophila*. After delamination from the neuroectoderm, each neuroblast goes through different phases of gene expression that confer temporal identity in the absence of extrinsic cues. Since the progeny maintain the temporal expression profile, the ventral neuromeres are subdivided into apico-basal layers, corresponding to the time of delamination, with different neural identities. Based on our expression data, we suggest a model in which in contrast, in *S. maritima*, *hunchback* and *Krüppel* are expressed in subsets of neural precursors generating *areas* with different temporal expression domains within the plane of the neuroectoderm. This expression pattern indicates that temporal changes in (extrinsic) spatial patterning cues result in the ordered definition of different neural identities. We suggest that the change in the mechanism of temporal identity specification has evolved in parallel with changes in the rate of embryonic development and in neuroectodermal cell number. Neurogen-

esis in *Drosophila* occurs during a very short time window (4 h), while in chelicerates and myriapods, neural precursor groups arise over several days, of a several week long embryogenesis (Stollewerk et al., 2001; Dove and Stollewerk, 2003; Kadner and Stollewerk, 2004; this study). In contrast to *Drosophila*, the ventral neuroectoderm of both chelicerates and myriapods consists of many small cells. In addition, most of the cell divisions occur in the surface layer in chelicerates and myriapods. Since the temporal identity genes cannot operate in postmitotic cells (Pearson and Doe, 2003), it can be assumed that neural precursor diversity is mainly generated in the neuroectoderm.

It is obvious that the long phase of neurogenesis leaves enough time for changing signaling cues to confer different spatial and temporal identities to neural precursors within the ventral neuroectoderm of these organisms (Stollewerk and Simpson, 2005). The spatial separation of these mechanisms in *Drosophila* allows a parallel specification of different neural precursor identities: neuroblasts escape the spatial signaling events in the neuroectoderm by delamination and independently produce progeny with specific temporal identities in the basal cell layers. This application of spatial and temporal mechanisms can operate in embryos with few neuroectodermal cells and a short duration of neurogenesis as seen in *Drosophila*.

Here, we show for the first time in an arthropod other than *Drosophila* that *hunchback* and *Krüppel* are expressed in a time-dependent manner in different subsets of neural precursors. We assume that cell cycle-independent temporal patterning mechanisms operating in the plane of the neuroepithelium were present in the last common ancestor of arthropods. Future studies of the expression pattern of *Pdm* and *castor*, and functional analyses that make use of molecular markers to distinguish between different precursor identities will show to what degree the genetic network conferring temporal identity in *Drosophila* is conserved in other arthropods.

Acknowledgments

We thank Michael Akam and Pat Simpson for providing support and lab space. Thanks to Wallace Arthur and Carlo Brena for participating in embryo collection. Adrian Friday helped with the analysis of the *Strigamia maritima Notch* sequence, and with the identification of specific homologies. We are grateful to Pat Simpson, Michael Akam, Savita Ayyar, and Sylvain Marcellini for critical comments on the manuscript. This project was funded by the Deutsche Forschungsgemeinschaft (A.S.) and the Wellcome Trust (P.S.). A.D.C. was funded by a FEBS long-term research fellowship and by BBSRC.

References

Bate, M., 1976. Embryogenesis of an insect nervous system: I. A map of thoracic and abdominal neuroblasts in *Locusta migratoria*. J. Embryol. Exp. Morphol. 35, 107–123.

Broadus, J., Doe, C.Q., 1995. Evolution of neuroblast identity: seven-up and prospero expression reveal homologous and divergent neuroblast fates in *Drosophila* and *Schistocerca*. Development 121, 3989–3996.

Cabrera, C.V., 1990. Lateral inhibition and cell fate during neurogenesis in *Drosophila*: interactions between scute, Notch, Delta. Development 109, 733–742.

Cabrera, C.V., Martinez-Arias, A., Bate, M., 1987. The expression of three members of the achaete-scute gene complex correlates with neuroblast segregation in *Drosophila*. Cell 50, 425–433.

Chipman, A.D., Arthur, W., Akam, M., 2004a. A double segment periodicity underlies segment generation in centipede development. Curr. Biol. 14, 1250–1255.

Chipman, A.D., Arthur, W., Akam, M., 2004b. Early development and segment formation in the centipede, *Strigamia maritima* (Geophilomorpha). Evol. Dev. 6, 78–89.

Doe, C.Q., Goodman, C.S., 1992. Molecular markers for identified neuroblasts and ganglion mother cells in the *Drosophila* central nervous system. Development 116, 855–863.

Dove, H., Stollewerk, A., 2003. Comparative analysis of neurogenesis in the myriapod *Glomeris marginata* (Diplopoda) suggests more similarities to chelicerates than to insects. Development 130, 2161–2171.

Eriksson, B.J., Tait, N.N., Budd, G.E., 2003. Head development in the onychophoran *Euperipatoides kanangrensis* with particular reference to the central nervous system. J. Morphol. 255, 1–23.

Fay, D.S., Stanley, H.M., Han, M., Wood, W.B., 1999. A *Caenorhabditis elegans* homologue of hunchback is required for late stages of development but not early embryonic patterning. Dev. Biol. 205, 240–253.

Friedrich, M., Tautz, D., 1995. Ribosomal DNA phylogeny of the major extant arthropod classes and the evolution of myriapods. Nature 376, 165–167.

Gerberding, M., 1997. Germ band formation and early neurogenesis of *Leptodora kindti* (Cladocera): first evidence for neuroblasts in the entomostracan crustaceans. Invertebr. Repord. Dev. 32, 73–93.

Goodman, C.S., Doe, C.Q., 1993. Embryonic development of the *Drosophila* central nervous system. In: Bate, M., Martinez-Arias, A. (Eds.), The Development of *Drosophila melanogaster*. Cold Spring Harbor Laboratory Press, New York, pp. 1131–1206.

Grosskortenhaus, R., Pearson, B.J., Marusich, A., Doe, C.Q., 2005. Regulation of temporal identity transitions in *Drosophila* neuroblasts. Dev. Cell 8, 193–202.

Hartenstein, V., Campos-Ortega, J.A., 1984. Early neurogenesis in wildtype *Drosophila melanogster*. Roux's Arch. Dev. Biol. 193, 308–325.

Harzsch, S., 2001. Neurogenesis in the crustacean ventral nerve cord: homology of neuron stem cells in *Malacostraca* and *Branchipoda*? Evol. Dev. 3, 154–169.

Harzsch, S., 2003. Ontogeny of the ventral nerve cord in malacostracan crustaceans: a common plan for neuronal development in Crustacea and Hexapoda? Arthropod. Struct. Dev. 32, 17–38.

Heitzler, P., Bourouis, M., Ruel, L., Carteret, C., Simpson, P., 1996. Genes of the Enhancer of split and achaete–scute complexes are required for a regulatory loop between Notch and Delta during lateral signalling in *Drosophila*. Development 122, 161–171.

Hülskamp, M., Pfeifle, C., Tautz, D., 1990. A morphogenetic gradient of Hunchback protein organizes the expression of the gap genes *Krüppel* and *knirps* in the early *Drosophila* embryo. Nature 346, 577–580.

Hwang, U.W., Friedrich, M., Tautz, D., Park, C.J., Kim, W., 2001. Mitochondrial protein phylogeny joins myriapods with chelicerates. Nature 413, 154–157.

Isshiki, T., Pearson, B., Holbrook, S., Doe, C.Q., 2001. *Drosophila* neuroblasts sequentially express transcription factors which specify the temporal identity of their neural progeny. Cell 106, 511–521.

Iwasa, J.H., Suver, D.W., Savage, R.M., 2000. The leech hunchback protein is expressed in the epithelium and CNS but not in the segmental precursor lineages. Dev. Genes Evol. 210, 277–288.

Jiménez, F., Campos-Ortega, J.A., 1979. A region of the *Drosophila* genome necessary for CNS development. Nature 282, 310–312.

Jiménez, F., Campos-Ortega, J.A., 1990. Defective neuroblast commitment in mutants of the achaete–scute complex and adjacent genes of *Drosophila melangaster*. Neuron 5, 81–89.

Kadner, D., Stollewerk, A., 2004. Neurogenesis in the chilopod *Lithobius forficatus* suggests more similarities to chelicerates than to insects. Dev. Genes Evol. 214 (8), 367–379.

Kambadur, R., Koizumi, K., Stivers, C., Nagle, J., Poole, S.J., Odenwald, W.F.,

1998. Regulation of POU genes by Castor and Hunchback establishes layered compartments in the *Drosophila* CNS. Genes Dev. 12, 246–260.
Kanai, M.I., Okabe, M., Hiromi, Y., 2005. Seven-up controls switching of transcription factors that specify temporal identities of *Drosophila* neuroblasts. Dev. Cell 8, 203–213.
Kusche, K., Burmester, T., 2001. Diplopod hemocyanin sequence and the phylogenetic position of the Myriapoda. Mol. Biol. Evol. 18, 1566–1573.
Ligoxygakis, P., Yu, S.Y., Delidakis, C., Baker, N.E., 1998. A subset of Notch functions during *Drosophila* eye development require Su(H) and E(spl) gene complex. Development 125, 2893–2900.
Mallatt, J.M., Garey, J.R., Shultz, J.W., 2004. Ecdysozoan phylogeny and Bayesian inference: first use of nearly complete 28S and 18S rRNA gene sequences to classify the arthropods and their kin. Mol. Phylogenet. Evol. 31, 178–191.
Martin-Bermudo, M.D., Martinez, C., Rodriguez, A., Jimenez, F., 1991. Distribution and function of the lethal of scute gene during early neurogenesis in *Drosophila*. Development 113, 445–454.
Martin-Bermudo, M.D., Carmena, A., Jimenez, F., 1995. Neurogenic genes control gene expression at the transcriptional level in early neurogenesis and in mesectoderm specification. Development 121, 219–224.
Nakao, K., Campos-Ortega, J.A., 1996. Persistent expression of genes of the Enhancer of split complex suppresses neural development in *Drosophila*. Neuron 16, 275–286.
Nardi, F., Spinsanti, G., Boore, J.L., Carapelli, A., Dallai, R., Frati, F., 2003. Hexapod origins: monophyletic or paraphyletic? Science 299, 1887–1889.
Novotny, T., Eiselt, R., Urban, J., 2002. Hunchback is required for specification of the early sublineage of neuroblast 7–3 in the *Drosophila* central nervous system. Development 129, 1027–1036.
Patel, N.H., Hayward, D.C., Lall, S., Pirkl, N.R., DiPietro, D., Ball, E.E., 2001. Grasshopper hunchback expression reveals conserved and novel aspects of axis formation and segmentation. Development 128, 3459–3472.
Pearson, B.J., Doe, C.Q., 2003. Regulation of neuroblast competence in *Drosophila*. Nature 425, 568–569.
Pisani, D., Poling, L.L., Lyons-Weiler, M., Hedges, B., 2004. The colonization of land by animals: molecular phylogeny and divergence times among arthropods. BMC Biol. 2, 1.
Romani, S., Campuzano, S., Modolell, J., 1987. The achaete–scute complex is expressed in neurogenic regions of *Drosophila* embryos. EMBO J. 6, 2085–2092.
Savage, R.M., Shankland, M., 1996. Identification and characterization of a *hunchback* orthologue, *Lzf2*, and its expression during leech embryogenesis. Dev. Biol. 175, 205–217.
Scholtz, G., 1992. Cell lineage studies in the crayfish *Cherax destructor* (Crustacea, Decapoda): germ band formation, segmentation and early neurogenesis. Roux's Arch. Dev. Biol. 202, 36–48.
Schulz, C., Tautz, D., 1994. Autonomous concentration-dependent activation and repression of Krüppel by hunchback in the *Drosophila* embryo. Development 120, 3043–3049.
Seugnet, L., Simpson, P., Haenlin, M., 1997. Transcriptional regulation of Notch and Delta: requirement for neuroblast segregation. Development 124, 2015–2025.
Simpson, P., 1990. Lateral inhibition and the development of the sensory bristles of the peripheral nervous system. Development 109, 509–519.
Skeath, J.B., 1999. At the nexus between pattern formation and cell-type specification: the generation of individual neuroblast fates in the *Drosophila* embryonic central nervous system. BioEssays 21, 922–931.
Skeath, J.B., Panganiban, J.S., Carroll, S.B., 1992. Gene regulation in two dimensions: the proneural *achaete* and *scute* genes are controlled by combinations of axis patterning genes through a common intergenic control region. Genes Dev. 6, 2606–2619.
Sommer, R., Tautz, D., 1991. Segmentation gene expression in the housefly *Musca domestica*. Development 113, 419–430.
Sommer, R., Retzlaff, M., Goerlich, K., Sander, K., Tautz, D., 1992. Evolutionary conservation pattern of zinc-finger domains of *Drosophila* segmentation genes. Proc. Natl. Acad. Sci. 89, 10782–10786.
Stollewerk, A., 2000. Changes in cell shape in the ventral neuroectoderm of *Drosophila melanogaster* depend on the activity of the achaete–scute complex genes. Dev. Genes Evol. 210, 190–199.
Stollewerk, A., 2002. Recruitment of cell groups through Delta/Notch signalling during spider neurogenesis. Development 129, 5339–5348.
Stollewerk, A., Chipman, A.D.C., in press. Neurogenesis in myriapods and chelicerates and its importance for understanding arthropod relationships. ICB (Integrated and Comparative Biology).
Stollewerk, A., Simpson, P., 2005. Evolution of early development of the nervous system: a comparison between arthropods. BioEssays 27, 874–883.
Stollewerk, A., Klämbt, C., Cantera, R., 1996. Electron microscopic analysis of midline glial cell development during embryogenesis and larval development using β-galactosidase expression as endogenous marker. Microsc. Res. Tech. 35, 294–306.
Stollewerk, A., Weller, M., Tautz, D., 2001. Neurogenesis in the spider *Cupiennius salei*. Development 128, 2673–2688.
Stollewerk, A., Tautz, D., Weller, M., 2003. Neurogenesis in the spider: new insights from comparative analysis of morphological processes and gene expression patterns. Arthropod Struct. Develop. 32, 5–16.
Wheeler, S.R., Skeath, J.B., 2005. The identification and expression of achaete–scute genes in the branchiopod crustacean *Triops longicaudatus*. Gene Expression Patterns 5, 695–700.
Wheeler, S.R., Carrico, M.L., Wilson, B.A., Brown, S.J., Skeath, J.B., 2003. The expression and function of the achaete–scute genes in *Tribolium castaneum* reveals conservation and variation in neural pattern formation and cell fate specification. Development 130, 4373–4381.
Withington, P.M., 2004. The development of the crustacean nervous system. In: Scholtz, G. (Ed.), Evolutionary Developmental Biology of Crustacea, Crustacean Issues vol. 15. Publishers A.A. Balkema, Lisse Netherlands, pp. 135–167.
Wolf, C., Schuh, R., 2000. Single mesodermal cells guide outgrowth of ectodermal tubular structures in *Drosophila*. Genes Dev. 14, 2140–2145.
Wolff, C., Sommer, R., Schröder, R., Glaser, G., Tautz, D., 1995. Conserved and divergent expression aspects of the *Drosophila* segmentation gene hunchback in the short germ band embryo of the flour beetle Tribolium. Development 121, 4227–4236.
Wu, X., Vasisht, V., Kosman, D., Reinitz, J., Small, S., 2001. Thoracic patterning by the *Drosophila* gap gene hunchback. Dev. Biol. 237, 79–92.
Zajac, M., Jones, G.L., Glazier, J.A., 2003. Simulating convergent extension by way of anisotropic differential adhesion. J. Theor. Biol. 222, 247–259.